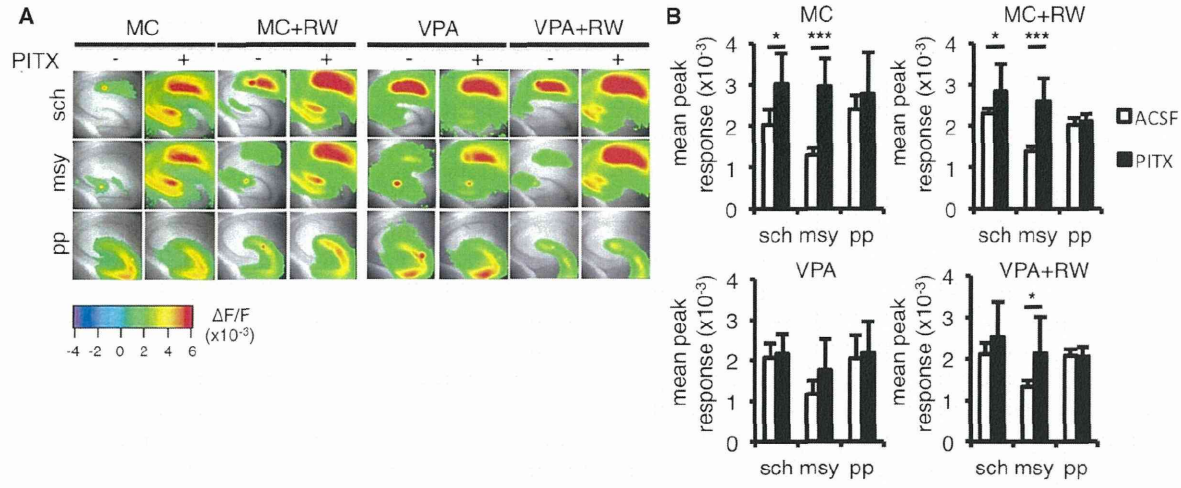

Figure 7. Voluntary Running Restores Neuronal Activity in VPA-Treated Mice

(A) Representative pseudocolor activity map images of brain slices including the hippocampus show that voluntary running can only recover the impairment of $GABA_A$ receptor-mediated inhibition in the mossy fiber pathway (msy) of VPA-treated mice, after treatment with the $GABA_A$ receptor channel antagonist picrotoxin (PITX) (n = 6 for MC, n = 9 for MC + RW, n = 7 for VPA, n = 8 for VPA + RW). Electrical stimulation was applied to Schaffer collateral afferents at the CA3/CA1 border of CA1 (sch); to the granule cell layer to stimulate the mossy fiber pathway (msy); and to the molecular layer of the upper blade in the DG (pp).

(B) Quantification of the neural response in artificial cerebrospinal fluid (ACSF), with (black bars) or without PITX (white bars; n = 6 for MC, n = 9 for MC + RW, n = 7 for VPA, n = 8 for VPA + RW). Note that although the augmentation of the neural response caused by $GABA_A$ receptor-mediated inhibition with PITX application seen in sch and msy was abolished in VPA-treated mice, voluntary running could restore the augmentation only in the msy.

MC, prenatal methylcellulose (vehicle); MC + RW, prenatal methylcellulose and postnatal running; VPA, prenatal valproic acid; VPA + RW, prenatal valproic acid and postnatal running. Data are represented as means. Error bars indicate the SD. $^*p < 0.05$, $^{***}p < 0.001$, two-tailed t test.

Voluntary Running Cannot Mitigate Abnormal Neuronal Morphology or Function of the Hippocampal CA1 Region in VPA-Treated Mice

The freezing response in the contextual fear test after voluntary running by VPA-treated mice did not recover to the level displayed by MC-treated mice (Figures 4G and S4D; Table S2). It has been proposed that recall of contextual memories relies more on CA1 than other regions in the hippocampus (Hall et al., 2001). Indeed, we found that apical dendrite morphology was abnormal in CA1 neurons of VPA-treated mice, and this defect was not repaired by voluntary running (Figures 5C, 5H, and 5I). Moreover, when we examined the region-specific restoration by voluntary running of neuronal activity in the hippocampus, the basal neuronal responses upon electrical stimulation were not affected by VPA nor voluntary running in the three major synaptic connections in the hippocampus (CA3-CA1, Schaffer collateral afferent [sch]; DG-CA3, mossy fiber [msy]; EC-DG, perforant pathway [pp]) possibly due to some homeostatic balancing mechanism (Turrigiano and Nelson, 2004; Turrigiano, 2011). However, when the excitatory activity was measured, with the increase in activity caused by an inhibitor for $GABA_A$ receptor picrotoxin (PITX) application, the effect of VPA became apparent. That is, the PITX induced an increase in sch and msy in MC-treated mice, which was not seen in VPA-treated mice, suggesting the impairment of inhibitory action in VPA-mice. The voluntary running could restore the characteristics only in msy (Figure 7). These results may explain why the recovery of neurogenesis and neuronal morphology of the DG in VPA-treated mice could not ameliorate their poor performance in the contextual associative test. Previous studies have indicated that ablation of adult neurogenesis in the DG leads to defective performance in a contextual associative test (Saxe et al., 2006; Wojtowicz et al., 2008) (but see Shors et al., 2002), but enhanced neurogenesis or running was weakly related to the performance in the test (Wojtowicz et al., 2008).

DISCUSSION

The precise pathology underlying postnatal impairment of cognitive function in children of epileptic expectant mothers treated with VPA, commonly used AED, is

unknown. Based on our findings in mice, we propose that the impairment is attributable to the untimely enhancement of embryonic neurogenesis, which leads to depletion of the NPC pool and consequently to a decreased level of postnatal neurogenesis in the hippocampus. Children of epileptic expectant mothers treated with VPA may also have hippocampal neurons with abnormal morphology and activity, as were observed in this study. Although prenatal exposure to AEDs such as VPA may have detrimental effects that persist until adulthood, we suggest that these effects could be mitigated by a simple physical activity such as running. Our results thus offer a straightforward strategy to help children born to epileptic mothers.

The cognitive deficits associated with prenatal VPA exposure might not due solely to the reduced neurogenesis with the abnormal neuronal morphology in the hippocampus, and there is a possibility that the low freezing responses in fear associative tests were contributed by the deficiency in amygdala, nociception, and/or motoric functions. Nevertheless, our data suggested that the reduced neurogenesis associated with the abnormal neuronal morphology in the hippocampus were very likely to be correlated with the observed cognitive deficits for several reasons. First, voluntary running is well known for its effect on enhancing both adult neurogenesis in the DG of the hippocampus and hippocampus-dependent learning and memory (Zhao et al., 2008), and this voluntary running could recover the cognitive deficit, if not all, in VPA-treated mice with reduced neurogenesis in the DG. Second, to the best of our knowledge, there are no reports to date that show a direct contribution of voluntary running to the enhancement of amygdala function that subsequently leads to an improvement in the cued fear response. Third, based on experiments that we have conducted, we could not find any significant differences in amygdala size and in the expression levels of cortical layer-specific genes of MC- and VPA-treated mice, with or without voluntary running. Fourth, total traveled distance in the open field, elevated plus and the Y-maze tests, and the number of light/dark transitions were not significantly different between MC- and VPA-treated mice, although in our earlier experiment some of these parameters showed modest differences. Moreover, in fear associative test, VPA-treated mice move similarly to MC-treated mice before the start of the tone (pre-tone), which indicate that motor deficiency is unlikely to be the main cause of low freezing responses in VPA-treated mice. Fifth, MC- and VPA-treated mice have similar basal nociceptive response and startle response to electric footshock during the conditioning for fear-associative test, thus it seems unlikely that VPA-treated mice have abnormal nociception and cannot sense the foot shock. Taking these facts into consideration, we therefore suggested that the reduced neurogenesis associated with the abnormal neuronal morphology in the hippocampus were very likely to be a critical cause of the observed cognitive deficits. However, we still cannot completely exclude the possibility that changes in other brain areas may also contribute to the deficits, warranting further future investigation.

We and others have shown previously that VPA treatment induces neuronal differentiation but suppresses glial differentiation of cultured multipotent NPCs (Hsieh et al., 2004; Balasubramaniyan et al., 2006; Murabe et al., 2007; Abematsu et al., 2010; Juliandi et al., 2012). We have now demonstrated that VPA also increases histone acetylation in the embryonic forebrain and induces neuronal differentiation of embryonic NPCs. Previous study have shown that VPA promotes neuronal differentiation by increasing histone H4 acetylation at proneural gene promoters (Yu et al., 2009). However, several studies have suggested that the activation of GSK-3β/β-catenin and/or ERK pathway is the main cause for the increase neurogenesis of NPCs by VPA (Yuan et al., 2001; Jung et al., 2008; Hao et al., 2004; Go et al., 2012). It has been suggested that VPA might have various cellular effects that will depend on the context of VPA usage and/or cell type and experimental design used in the study, which warrant further research to reveal the connection between these effects (Kostrouchová et al., 2007; Rosenberg, 2007).

We suggest that gene expression change caused by VPA is attributable mainly to its HDAC-inhibiting activity. To date, more than a dozen HDACs have been characterized and they are classified into at least three major groups. In particular, HDAC1 and HDAC2, belonging to the class I group, have been reported to regulate NPC differentiation (Sun et al., 2011). NPCs express high levels of HDAC1 and some of them also express low levels of HDAC2 (MacDonald and Roskams, 2008). Interestingly, as NPCs are committed to the neuronal lineage, expression of HDAC2 is upregulated while that of HDAC1 is downregulated and becomes undetectable in most post-mitotic neurons (MacDonald et al., 2005; MacDonald and Roskams, 2008); on the other hand, HDAC1 expression is sustained in the majority of cells in glial lineages (astrocytes and oligodendrocytes), in which HDAC2 is not detected (Shen et al., 2005; MacDonald and Roskams, 2008). Moreover, HDAC2, but not HDAC1, was found to inhibit astrocytic differentiation (Humphrey et al., 2008). Therefore, although VPA is capable of inhibiting both HDAC1 and HDAC2 (Kazantsev and Thompson, 2008), it is tempting to speculate that the main target of VPA in HDAC inhibition-mediated neuronal differentiation of NPCs is HDAC1. It will be of interest to explore this possibility in a future study.

Neurogenesis in the adult mammalian brain occurs throughout life and has been clearly demonstrated at two

locations under physiological conditions: the SVZ of the lateral ventricle and the subgranular zone (SGZ) of the DG in the hippocampus (Alvarez-Buylla and Lim, 2004). Several studies have shown that hippocampal neurogenesis is regulated by both physiological and pathological activities at different stages, including (1) proliferation of NPCs, (2) fate determination and differentiation of NPCs, and (3) survival, maturation, and integration of newborn neurons (Zhao et al., 2008). Furthermore, each of these stages is subject to regulation by numerous intrinsic and extrinsic factors (Suh et al., 2009). Genetic and environmental factors that affect adult hippocampal neurogenesis also cause alteration in cognitive performance, suggesting roles for adult hippocampal neurogenesis in learning and memory (Zhao et al., 2008). Our results showed that VPA-treated mice have a decreased level of postnatal neurogenesis in the hippocampus, which correlates with their poor performance in learning and memory tests. We have shown here and elsewhere (Hsieh et al., 2004; Jessberger et al., 2007) that VPA can reduce the proliferation of NPCs, and this reduction, together with the enhancement of neurogenesis, probably led to the depletion of the NPC pool in VPA-treated mice. It is possible that this depletion caused a slower differentiation of the residual NPCs in order to maintain required number of NPC pool during life. This possibility is an interesting avenue to be explored in the future.

In accordance with previous studies (van Praag et al., 1999a, 1999b), we found that voluntary running augments hippocampal neurogenesis of both MC- and VPA-treated mice, and it restores learning and memory deficiencies in VPA-treated mice. A previous report has shown the same restoration of decreased hippocampal neurogenesis and learning deficits in aged rodents by voluntary running (van Praag et al., 2005), although the precise molecular mechanisms responsible for voluntary running-induced neurogenesis remain undetermined (Deng et al., 2010). Here, we propose that at least the increase expression level of *Bdnf*, and the reduction of activated microglia may contribute to the restoration of impaired hippocampal neurogenesis and neuronal morphology in the DG of VPA-treated mice after voluntary running. However, future exploration is necessary to reveal the direct connection between the increase expression level of *Bdnf* and the reduction of microglia and its activated form in the hippocampus after voluntary running.

EXPERIMENTAL PROCEDURES

Animal Treatment

All experiments were carried out according to institutional animal experimentation guidelines, which comply with the NIH Guide for Care and Use of Laboratory Animals. All efforts were made to minimize the number of animals used and their suffering. Pregnant C57BL/6 mice were individually housed in plastic breeding cages with free access to water and pellet diet in a 12-hr light-dark cycle. For a detailed description of groups and treatments, see the Supplemental Experimental Procedures.

Immunohistochemistry, Nissl, and Golgi Staining

Mice were anesthetized and perfused with PBS followed by 4% PFA in PBS. The brain was dissected, postfixed, and processed for immunohistochemistry. For Nissl staining, brain sections were defatted with xylene, hydrated through a graded ethanol series (100%, 95%, and 70%), and washed with water before stained with 0.2% thionin solution (pH 4.0). Sections were then dehydrated in water and a graded ethanol series (70%, 95%, and 100%), clear in xylene, and mounted with Entellan (Merck). For Golgi staining, the brain was removed from the skull without any perfusion and then sectioned (100 μm) on a cryostat. For a more detailed description and list of antibodies, see the Supplemental Experimental Procedures.

Measurement and Morphometrics

For a detailed description of cell count, volume measurement and cell/tissue morphometrics, see the Supplemental Experimental Procedures.

Gene Expression Analysis

For a detailed description of GeneChip and real-time qPCR procedures, see the Supplemental Experimental Procedures.

Behavioral Tests

Behavioral experiments were performed sequentially using male mice. For a more detailed description, see the Supplemental Experimental Procedures.

Voltage-Sensitive Dye Imaging

Experiment was done using hippocampal slices. For a more detailed description, see the Supplemental Experimental Procedures.

Statistics

Statistical analyses were performed by Student's two-tailed t test (unpaired) and one-way or two-way ANOVA using R software (http://www.r-project.org) (n indicates individual mice).

ACCESSION NUMBERS

The accession number for the GeneChip data reported in this paper is GEO: GSE42904.

SUPPLEMENTAL INFORMATION

Supplemental Information includes Supplemental Experimental Procedures, five figures, and two tables and can be found with this article online at http://dx.doi.org/10.1016/j.stemcr.2015.10.012.

AUTHOR CONTRIBUTIONS

B.J. and K.N. conceived and designed the study. B.J., K. Tanemura, K.I., T.T., Y.F., M.O.I., N.M., and D.I. carried out the experiments. B.J., K. Tanemura, K.I., T.T., M.A., T.S., K. Tsujimura, M.N., and K.N. analyzed the data. J.K. supported the experiments. B.J. and K.N. wrote the manuscript.

ACKNOWLEDGMENTS

We thank Y. Bessho, T. Matsui, Y. Nakahata, J. Kohyama, T. Takizawa, M. Namihira, S. Katada, and T. Imamura for valuable discussions. We also thank I. Smith for critical reading of the manuscript. We are very grateful to M. Tano for her excellent secretarial assistance and other laboratory members for discussion and technical help. This research was supported in part by the NAIST Global COE Program (Frontier Biosciences: Strategies for survival and adaptation in a changing global environment) from the Ministry of Education, Culture, Sports, Science and Technology of Japan (MEXT); a Grant-in-Aid for Scientific Research on Innovative Area: Neural Diversity and Neocortical Organization from MEXT; Health Sciences Research Grants from the Ministry of Health, Labour and Welfare, Japan; Core Research for Evolutional Science and Technology (CREST) from the Japan Science and Technology Corporation; and Research Fellowships for Young Scientists from the Japan Society for the Promotion of Science.

Received: June 24, 2015
Revised: October 22, 2015
Accepted: October 23, 2015
Published: November 19, 2015

REFERENCES

Abematsu, M., Tsujimura, K., Yamano, M., Saito, M., Kohno, K., Kohyama, J., Namihira, M., Komiya, S., and Nakashima, K. (2010). Neurons derived from transplanted neural stem cells restore disrupted neuronal circuitry in a mouse model of spinal cord injury. J. Clin. Invest. *120*, 3255–3266.

Alvarez-Buylla, A., and Lim, D.A. (2004). For the long run: maintaining germinal niches in the adult brain. Neuron *41*, 683–686.

Balasubramaniyan, V., Boddeke, E., Bakels, R., Küst, B., Kooistra, S., Veneman, A., and Copray, S. (2006). Effects of histone deacetylation inhibition on neuronal differentiation of embryonic mouse neural stem cells. Neuroscience *143*, 939–951.

Battino, D., and Tomson, T. (2007). Management of epilepsy during pregnancy. Drugs *67*, 2727–2746.

Bekinschtein, P., Oomen, C.A., Saksida, L.M., and Bussey, T.J. (2011). Effects of environmental enrichment and voluntary exercise on neurogenesis, learning and memory, and pattern separation: BDNF as a critical variable? Semin. Cell Dev. Biol. *22*, 536–542.

Blaheta, R.A., and Cinatl, J., Jr. (2002). Anti-tumor mechanisms of valproate: a novel role for an old drug. Med. Res. Rev. *22*, 492–511.

Chang, B.S., and Lowenstein, D.H. (2003). Epilepsy. N. Engl. J. Med. *349*, 1257–1266.

Deng, W., Aimone, J.B., and Gage, F.H. (2010). New neurons and new memories: how does adult hippocampal neurogenesis affect learning and memory? Nat. Rev. Neurosci. *11*, 339–350.

DiLiberti, J.H., Farndon, P.A., Dennis, N.R., and Curry, C.J. (1984). The fetal valproate syndrome. Am. J. Med. Genet. *19*, 473–481.

Farmer, J., Zhao, X., van Praag, H., Wodtke, K., Gage, F.H., and Christie, B.R. (2004). Effects of voluntary exercise on synaptic plasticity and gene expression in the dentate gyrus of adult male Sprague-Dawley rats in vivo. Neuroscience *124*, 71–79.

Gebara, E., Sultan, S., Kocher-Braissant, J., and Toni, N. (2013). Adult hippocampal neurogenesis inversely correlates with microglia in conditions of voluntary running and aging. Front. Neurosci. *7*, 145.

Go, H.S., Kim, K.C., Choi, C.S., Jeon, S.J., Kwon, K.J., Han, S.H., Lee, J., Cheong, J.H., Ryu, J.H., Kim, C.H., et al. (2012). Prenatal exposure to valproic acid increases the neural progenitor cell pool and induces macrocephaly in rat brain via a mechanism involving the GSK-3β/β-catenin pathway. Neuropharmacology *63*, 1028–1041.

Göttlicher, M., Minucci, S., Zhu, P., Krämer, O.H., Schimpf, A., Giavara, S., Sleeman, J.P., Lo Coco, F., Nervi, C., Pelicci, P.G., and Heinzel, T. (2001). Valproic acid defines a novel class of HDAC inhibitors inducing differentiation of transformed cells. EMBO J. *20*, 6969–6978.

Hall, J., Thomas, K.L., and Everitt, B.J. (2001). Cellular imaging of zif268 expression in the hippocampus and amygdala during contextual and cued fear memory retrieval: selective activation of hippocampal CA1 neurons during the recall of contextual memories. J. Neurosci. *21*, 2186–2193.

Hao, Y., Creson, T., Zhang, L., Li, P., Du, F., Yuan, P., Gould, T.D., Manji, H.K., and Chen, G. (2004). Mood stabilizer valproate promotes ERK pathway-dependent cortical neuronal growth and neurogenesis. J. Neurosci. *24*, 6590–6599.

Hsieh, J., Nakashima, K., Kuwabara, T., Mejia, E., and Gage, F.H. (2004). Histone deacetylase inhibition-mediated neuronal differentiation of multipotent adult neural progenitor cells. Proc. Natl. Acad. Sci. USA *101*, 16659–16664.

Humphrey, G.W., Wang, Y.H., Hirai, T., Padmanabhan, R., Panchision, D.M., Newell, L.F., McKay, R.D., and Howard, B.H. (2008). Complementary roles for histone deacetylases 1, 2, and 3 in differentiation of pluripotent stem cells. Differentiation *76*, 348–356.

Jessberger, S., Nakashima, K., Clemenson, G.D., Jr., Mejia, E., Mathews, E., Ure, K., Ogawa, S., Sinton, C.M., Gage, F.H., and Hsieh, J. (2007). Epigenetic modulation of seizure-induced neurogenesis and cognitive decline. J. Neurosci. *27*, 5967–5975.

Joint Epilepsy Council (2011). Epilepsy Prevalence, Incidence, and Other Statistic (Joint Epilepsy Council Publication).

Juliandi, B., Abematsu, M., Sanosaka, T., Tsujimura, K., Smith, A., and Nakashima, K. (2012). Induction of superficial cortical layer neurons from mouse embryonic stem cells by valproic acid. Neurosci. Res. *72*, 23–31.

Jung, G.A., Yoon, J.Y., Moon, B.S., Yang, D.H., Kim, H.Y., Lee, S.H., Bryja, V., Arenas, E., and Choi, K.Y. (2008). Valproic acid induces differentiation and inhibition of proliferation in neural progenitor

cells via the beta-catenin-Ras-ERK-p21Cip/WAF1 pathway. BMC Cell Biol. *9*, 66.

Kazantsev, A.G., and Thompson, L.M. (2008). Therapeutic application of histone deacetylase inhibitors for central nervous system disorders. Nat. Rev. Drug Discov. *7*, 854–868.

Kohman, R.A., Bhattacharya, T.K., Wojcik, E., and Rhodes, J.S. (2013). Exercise reduces activation of microglia isolated from hippocampus and brain of aged mice. J. Neuroinflammation *10*, 114.

Kostrouchová, M., Kostrouch, Z., and Kostrouchová, M. (2007). Valproic acid, a molecular lead to multiple regulatory pathways. Folia Biol. (Praha) *53*, 37–49.

LeDoux, J. (2003). The emotional brain, fear, and the amygdala. Cell. Mol. Neurobiol. *23*, 727–738.

MacDonald, J.L., and Roskams, A.J. (2008). Histone deacetylases 1 and 2 are expressed at distinct stages of neuro-glial development. Dev. Dyn. *237*, 2256–2267.

MacDonald, J.L., Gin, C.S., and Roskams, A.J. (2005). Stage-specific induction of DNA methyltransferases in olfactory receptor neuron development. Dev. Biol. *288*, 461–473.

Matsuda, T., Murao, N., Katano, Y., Juliandi, B., Kohyama, J., Akira, S., Kawai, T., and Nakashima, K. (2015). TLR9 signalling in microglia attenuates seizure-induced aberrant neurogenesis in the adult hippocampus. Nat. Commun. *6*, 6514.

Meador, K.J., Baker, G.A., Browning, N., Clayton-Smith, J., Combs-Cantrell, D.T., Cohen, M., Kalayjian, L.A., Kanner, A., Liporace, J.D., Pennell, P.B., et al.; NEAD Study Group (2009). Cognitive function at 3 years of age after fetal exposure to antiepileptic drugs. N. Engl. J. Med. *360*, 1597–1605.

Meador, K.J., Baker, G.A., Browning, N., Cohen, M.J., Clayton-Smith, J., Kalayjian, L.A., Kanner, A., Liporace, J.D., Pennell, P.B., Privitera, M., and Loring, D.W.; NEAD Study Group (2011). Foetal antiepileptic drug exposure and verbal versus non-verbal abilities at three years of age. Brain *134*, 396–404.

Meador, K.J., Baker, G.A., Browning, N., Cohen, M.J., Bromley, R.L., Clayton-Smith, J., Kalayjian, L.A., Kanner, A., Liporace, J.D., Pennell, P.B., et al.; NEAD Study Group (2012). Effects of fetal antiepileptic drug exposure: outcomes at age 4.5 years. Neurology *78*, 1207–1214.

Meador, K.J., Baker, G.A., Browning, N., Cohen, M.J., Bromley, R.L., Clayton-Smith, J., Kalayjian, L.A., Kanner, A., Liporace, J.D., Pennell, P.B., et al.; NEAD Study Group (2013). Fetal antiepileptic drug exposure and cognitive outcomes at age 6 years (NEAD study): a prospective observational study. Lancet Neurol. *12*, 244–252.

Meinardi, H., Scott, R.A., Reis, R., and Sander, J.W.; ILAE Commission on the Developing World (2001). The treatment gap in epilepsy: the current situation and ways forward. Epilepsia *42*, 136–149.

Molyneaux, B.J., Arlotta, P., Menezes, J.R., and Macklis, J.D. (2007). Neuronal subtype specification in the cerebral cortex. Nat. Rev. Neurosci. *8*, 427–437.

Murabe, M., Yamauchi, J., Fujiwara, Y., Hiroyama, M., Sanbe, A., and Tanoue, A. (2007). A novel embryotoxic estimation method of VPA using ES cells differentiation system. Biochem. Biophys. Res. Commun. *352*, 164–169.

Nau, H., Hauck, R.S., and Ehlers, K. (1991). Valproic acid-induced neural tube defects in mouse and human: aspects of chirality, alternative drug development, pharmacokinetics and possible mechanisms. Pharmacol. Toxicol. *69*, 310–321.

Ngugi, A.K., Bottomley, C., Kleinschmidt, I., Sander, J.W., and Newton, C.R. (2010). Estimation of the burden of active and lifetime epilepsy: a meta-analytic approach. Epilepsia *51*, 883–890.

Phiel, C.J., Zhang, F., Huang, E.Y., Guenther, M.G., Lazar, M.A., and Klein, P.S. (2001). Histone deacetylase is a direct target of valproic acid, a potent anticonvulsant, mood stabilizer, and teratogen. J. Biol. Chem. *276*, 36734–36741.

Rosenberg, G. (2007). The mechanisms of action of valproate in neuropsychiatric disorders: can we see the forest for the trees? Cell. Mol. Life Sci. *64*, 2090–2103.

Sander, J.W. (2003). The epidemiology of epilepsy revisited. Curr. Opin. Neurol. *16*, 165–170.

Sarnyai, Z., Sibille, E.L., Pavlides, C., Fenster, R.J., McEwen, B.S., and Tóth, M. (2000). Impaired hippocampal-dependent learning and functional abnormalities in the hippocampus in mice lacking serotonin(1A) receptors. Proc. Natl. Acad. Sci. USA *97*, 14731–14736.

Saxe, M.D., Battaglia, F., Wang, J.W., Malleret, G., David, D.J., Monckton, J.E., Garcia, A.D., Sofroniew, M.V., Kandel, E.R., Santarelli, L., et al. (2006). Ablation of hippocampal neurogenesis impairs contextual fear conditioning and synaptic plasticity in the dentate gyrus. Proc. Natl. Acad. Sci. USA *103*, 17501–17506.

Shen, S., Li, J., and Casaccia-Bonnefil, P. (2005). Histone modifications affect timing of oligodendrocyte progenitor differentiation in the developing rat brain. J. Cell Biol. *169*, 577–589.

Shors, T.J., Townsend, D.A., Zhao, M., Kozorovitskiy, Y., and Gould, E. (2002). Neurogenesis may relate to some but not all types of hippocampal-dependent learning. Hippocampus *12*, 578–584.

Sierra, A., Encinas, J.M., Deudero, J.J., Chancey, J.H., Enikolopov, G., Overstreet-Wadiche, L.S., Tsirka, S.E., and Maletic-Savatic, M. (2010). Microglia shape adult hippocampal neurogenesis through apoptosis-coupled phagocytosis. Cell Stem Cell *7*, 483–495.

Stranahan, A.M. (2011). Physiological variability in brain-derived neurotrophic factor expression predicts dendritic spine density in the mouse dentate gyrus. Neurosci. Lett. *495*, 60–62.

Suh, H., Deng, W., and Gage, F.H. (2009). Signaling in adult neurogenesis. Annu. Rev. Cell Dev. Biol. *25*, 253–275.

Sun, G., Fu, C., Shen, C., and Shi, Y. (2011). Histone deacetylases in neural stem cells and induced pluripotent stem cells. J. Biomed. Biotechnol. *2011*, 835968.

Tolwani, R.J., Buckmaster, P.S., Varma, S., Cosgaya, J.M., Wu, Y., Suri, C., and Shooter, E.M. (2002). BDNF overexpression increases dendrite complexity in hippocampal dentate gyrus. Neuroscience *114*, 795–805.

Turrigiano, G. (2011). Too many cooks? Intrinsic and synaptic homeostatic mechanisms in cortical circuit refinement. Annu. Rev. Neurosci. *34*, 89–103.

Turrigiano, G.G., and Nelson, S.B. (2004). Homeostatic plasticity in the developing nervous system. Nat. Rev. Neurosci. *5*, 97–107.

Van der Borght, K., Havekes, R., Bos, T., Eggen, B.J., and Van der Zee, E.A. (2007). Exercise improves memory acquisition and retrieval in the Y-maze task: relationship with hippocampal neurogenesis. Behav. Neurosci. *121*, 324–334.

van Praag, H. (2009). Exercise and the brain: something to chew on. Trends Neurosci. *32*, 283–290.

van Praag, H., Christie, B.R., Sejnowski, T.J., and Gage, F.H. (1999a). Running enhances neurogenesis, learning, and long-term potentiation in mice. Proc. Natl. Acad. Sci. USA *96*, 13427–13431.

van Praag, H., Kempermann, G., and Gage, F.H. (1999b). Running increases cell proliferation and neurogenesis in the adult mouse dentate gyrus. Nat. Neurosci. *2*, 266–270.

van Praag, H., Shubert, T., Zhao, C., and Gage, F.H. (2005). Exercise enhances learning and hippocampal neurogenesis in aged mice. J. Neurosci. *25*, 8680–8685.

van Strien, N.M., Cappaert, N.L., and Witter, M.P. (2009). The anatomy of memory: an interactive overview of the parahippocampal-hippocampal network. Nat. Rev. Neurosci. *10*, 272–282.

Vukovic, J., Colditz, M.J., Blackmore, D.G., Ruitenberg, M.J., and Bartlett, P.F. (2012). Microglia modulate hippocampal neural precursor activity in response to exercise and aging. J. Neurosci. *32*, 6435–6443.

Wojtowicz, J.M., Askew, M.L., and Winocur, G. (2008). The effects of running and of inhibiting adult neurogenesis on learning and memory in rats. Eur. J. Neurosci. *27*, 1494–1502.

Yang, R.J., Mozhui, K., Karlsson, R.M., Cameron, H.A., Williams, R.W., and Holmes, A. (2008). Variation in mouse basolateral amygdala volume is associated with differences in stress reactivity and fear learning. Neuropsychopharmacology *33*, 2595–2604.

Yu, I.T., Park, J.Y., Kim, S.H., Lee, J.S., Kim, Y.S., and Son, H. (2009). Valproic acid promotes neuronal differentiation by induction of proneural factors in association with H4 acetylation. Neuropharmacology *56*, 473–480.

Yuan, P.X., Huang, L.D., Jiang, Y.M., Gutkind, J.S., Manji, H.K., and Chen, G. (2001). The mood stabilizer valproic acid activates mitogen-activated protein kinases and promotes neurite growth. J. Biol. Chem. *276*, 31674–31683.

Zhao, C., Deng, W., and Gage, F.H. (2008). Mechanisms and functional implications of adult neurogenesis. Cell *132*, 645–660.

Nim et al. BMC Bioinformatics (2015) 16:141
DOI 10.1186/s12859-015-0578-0

BMC Bioinformatics

SOFTWARE Open Access

VISIONET: intuitive visualisation of overlapping transcription factor networks, with applications in cardiogenic gene discovery

Hieu T Nim[1,2*], Milena B Furtado[2], Mauro W Costa[2], Nadia A Rosenthal[1,2,3], Hiroaki Kitano[1,2,4,5] and Sarah E Boyd[1,2*]

Abstract

Background: Existing *de novo* software platforms have largely overlooked a valuable resource, the expertise of the intended biologist users. Typical data representations such as long gene lists, or highly dense and overlapping transcription factor networks often hinder biologists from relating these results to their expertise.

Results: VISIONET, a streamlined visualisation tool built from experimental needs, enables biologists to transform large and dense overlapping transcription factor networks into sparse human-readable graphs via numerically filtering. The VISIONET interface allows users without a computing background to interactively explore and filter their data, and empowers them to apply their specialist knowledge on far more complex and substantial data sets than is currently possible. Applying VISIONET to the Tbx20-Gata4 transcription factor network led to the discovery and validation of *Aldh1a2*, an essential developmental gene associated with various important cardiac disorders, as a healthy adult cardiac fibroblast gene co-regulated by cardiogenic transcription factors Gata4 and Tbx20.

Conclusions: We demonstrate with experimental validations the utility of VISIONET for expertise-driven gene discovery that opens new experimental directions that would not otherwise have been identified.

Keywords: Visualisation, Human-readable, Gene expression, Transcription factor, Network overlap

Background

A substantial body of computational research in biology is focused on building "*de novo* discovery platforms", *i.e.* software that draws statistical predictions from high-throughput experiments [1]. In contrast, typical analyses by experimental biologists exploit specialist knowledge and an ability to accurately judge the feasibility of *in vivo* laboratory validations. The complementary power of computing and human expertise [2] has promoted a new class of expertise-driven semi-automated computational tools [3], such as the image analysis platform CL-Quant by Nikon that has recently gained commercial and clinical success [4,5].

Experimental biologists are usually intimately familiar with a finite set of genes featured in their biological system of interest. Key regulatory genes have generally already been investigated and confirmed *in vivo*, but the relationship between those genes and the transcription factors that regulate their expression is often unknown [6]. Transcription factors often act in concert, forming tightly controlled networks, and many gene targets are shared among different transcription factors [7,8]. Identification of overlapping regulation of genes within transcription factor networks carries significant potential for untangling the complex biological processes being studied.

Data visualisation is one of the most powerful approaches designed to bridge the computational/experimental divide and facilitate biological discovery, in particular visualisation of gene regulatory networks, where novel systems-level properties can be inferred from the network characteristics [1,9]. However two major hurdles still persist for biologists; different types of -omics assays cannot be integrated, greatly limiting the utility for biologists [10], and the sheer scale of

* Correspondence: hieu.nim@monash.edu; sarah.boyd@monash.edu
[1]Systems Biology Institute (SBI) Australia, Monash University, Clayton, VIC 3800, Australia
[2]Australian Regenerative Medicine Institute, Monash University, Clayton, VIC 3800, Australia
Full list of author information is available at the end of the article

these the networks exceeds capacity for human interpretation [11].

We have encountered exactly this scenario in the field of cardiac research. The mammalian heart is a complex structure with highly specialised cells working under a tightly regulated environment [7,8]. To understand cardiac function and disease, the cardiovascular research community still largely uses conventional approaches (*e.g.* transgenic mice) and thus focuses on a small group of highly cardiac-specific genes [12]. Their data sets are generally very focussed, in-house, and specific to particular experimental conditions. Working hypotheses are generally based on the existing body of literature, on substantial in-house expertise, and on an experimental approach that is optimised for the research being undertaken within that group or laboratory. The missing link between their experimental research and computational approaches is a tool that facilitates mapping of gene expression data onto transcription factor networks.

We have therefore developed VISIONET, a tool to integrate transcription factor (TF) networks obtained from ChIP-seq studies with gene expression levels from microarray data. The purpose of this tool is to allow biologist users to apply domain expertise to reason about and explore the experimental data that they have generated. In particular, VISIONET is designed to reveal co-regulated genes that have strong expression signatures. Unlike other typical data-intensive tools for analysing ChIP-Seq or microarray data, VISIONET is specifically designed for biologists, with a web-based interactive graphical interface tailored to provide human-readable information, which filters the dense network according to gene expression levels and displays reduced quantities of information to facilitate direct interpretation by the expert users. We have also implemented customised layout algorithms that are specific for TF networks, and in particular overlapping TF networks, which are optimized for human readability. VISIONET is intended as a complementary tool to the existing large-scale discovery platforms such as Cytoscape and CellDesigner.

We illustrate the purpose and utility of our tool with a case study in which we have applied VISIONET to microarray results obtained in our recent investigation of TFs that regulate cardiac fibroblasts identity [13]. In the developing mouse heart, Tbx20 directly interacts with Gata4 to co-regulate the heart development program [14] and Tbx20-Gata4 co-regulated genes are increasingly important topics for systematic investigation [15]. We have revisited this dataset using VISIONET, to show that integrated visualisation of the Gata4 and Tbx20 TF networks allows rapid discovery of common co-regulated genes in the adult mouse cardiac fibroblasts. This approach has led to identification of *Aldh1a2*, a gene that already has a recognised role in cardiogenesis [16], and now from this study also appears to be highly up-regulated in adult cardiac fibroblasts.

Implementation

The design of the VISIONET system is based on satisfying the requirements of expertise-driven gene discovery, which requires all of the following features: overlaying gene expression data on top of transcription factor networks, layout methods tailored to visualising overlapping transcription factor networks, and numerically filtering for human readability. In our experience working in cardiac biology, these features (Figure 1A) are not all currently available in existing interactive visualisation platforms CellDesigner v4.4 [17], PAYAO [18], Cytoscape v2.8 [19], VisANT 4.0 [20], and WikiPathways [21]. In the specific case of TF network topology, currently it is not a trivial task to generate a readable network layout and apply numerical filtering using existing visualisation platforms. All existing platforms do not have specific layout method for overlapping TF network topology. Numerical filtering, if available (such as in Cytoscape) requires a substantial degree of user sophistication, much greater than the average level of a general biologist user.

The VISIONET web service was developed in the Microsoft ASP.NET environment using the open source NodeXL application programming interface [22]. The VISIONET pipeline (Figure 1B) has a back-end that handles the data integration and graph rendering from the transcriptomic datasets, and a front-end for biologist users that allows them to interactively control the display of the TF network. The node properties can be any numerical values that the biologist users are measuring (fold-change, *p*-values, RNA-Seq's reads per kilobase, *etc.*). Thus VISIONET enables users to address the overall biological question (gene discovery) and specific biological questions (genes having certain fold-changes, *p*-values, *etc.*). The biologist users can interact with the web-based graphical interface from most common browsers in at least two ways: by defining what properties to be associated with each node (fold-change, *p*-value of a *t*-test), and by specifying the cut-off for numerical filtering.. The network graphics are rendered in the *GIF* format, which has excellent compression ratio for images with few distinct colours.

Two input files are required: (1) the < *gene 1, gene 2* > tuples that describe the TF network, and (2) the < *gene, value* > tuples for the microarray intensity. Inputs (1) and (2) are provided in tab- or comma-separated format, and (1) also accepts *GraphML* format [23]. Alternatively, the user can supply the raw ChIP-Seq peak

A

Tool	Main Objective	Overlay gene expression data	Layout overlapping TF networks?	Numerical node filtering?
VISIONET	Expertise-driven gene target discovery from dense overlapping transcription factor networks	Yes	Yes	Yes
CellDesigner	Pathway construction and simulation	Yes (via plug-ins)	No	No
PAYAO	Community-driven pathway curation based on CellDesigner	No	No	No
Cytoscape	Molecular network visualisation	Yes (via plug-ins)	No	Yes (advanced users)
VisANT	Integrating genes, drugs, diseases and therapies	Yes	Partly	No
WikiPathways	Community-driven pathway curation based on Wiki platform	No	No	No

B

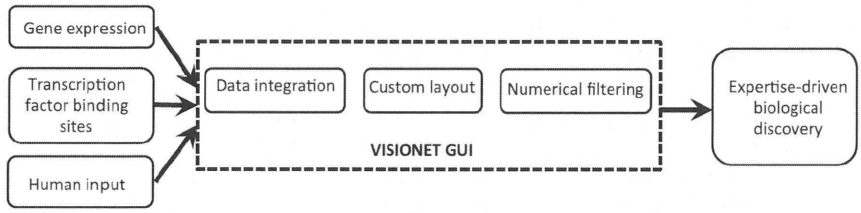

Figure 1 VISIONET implementation uniqueness. **(A)** Comparison of VISIONET features with popular biological network visualisation analysis tools. VISIONET implements five features to facilitate expertise-driven visualisation and analysis of overlapping transcription factor networks. Using empirical evaluation based on our case study, the availability of these features was assessed in the most popular existing tools: CellDesigner v4.4 [17], PAYAO [18], Cytoscape v2.8 [19], VisANT 4.0 [20], and WikiPathways [21]. **(B)** Schematic flowchart illustrating the architecture of VISIONET, designed to facilitate expertise-driven biological discovery. Gene expression and TF binding site data are supplied to VISIONET, and biologist interacts with VISIONET to determine which network components to display. Internally, VISIONET performs the computationally intensive task of data integration, graph layout and network filtering.

list for (1) in the standard *COD* format, and the raw microarray files for (2) in the standard *SOFT* format.

The filtering feature of VISIONET enables the user to control the visualisation of the network, so that only a small (relevant) sub-network of interest is displayed, while the remainder of the network is blurred or omitted. This feature is highly useful for biologists, as human inspection is feasible when only a small number of genes are visible at a time. Filtering is typically performed calculating the log fold change (Log FC) value of each gene based on the supplied transcriptomes to VISIONET. Optionally, other filtering criteria are possible by supplying VISIONET with a list of $< gene, value >$ tuples that represents any numerical property of the genes. Thus there are numerous use cases for VISIONET filtering function, such as "filter out all genes with Log FC value between −4 and 4", or "show only genes with p-value < 0.001 based on an unpaired t-test".

VISIONET has a customised layout algorithm that takes advantage of the topology of TF networks, where each edge connects a high-degreed node (TF) and numerous low-degreed nodes (target genes). In brief, the layout algorithm spaces the TFs equidistant from each other in a circle, and layout the target genes randomly in fixed-location boxes (Algorithm 1).

Algorithm 1. VISIONET layout algorithm designed for overlapping TF network topology. To improve human-readability, the VISIONET layout method emphasises the overlapping regions of the TF network by placing them in separate boxes.

1. Arrange all TFs equidistantly in a circle C of radius r
2. For each target gene g
2.1 Compute $\mathbf{S}(g)$, the set of TFs connected to g
2.2 If $\mathbf{S}(g)$ has size 1,
Place g randomly in a box with dimensions $r/2 \times r$ and centred outside C
2.3 Else if $\mathbf{S}(g)$ has size greater than 1
Place g randomly in a box with dimensions $r/\text{size}(\mathbf{S}(g)) \times r/\text{size}(\mathbf{S}(g))$ and centred at the centroid of $\mathbf{S}(g)$

The performance of the VISIONET web service depends on the number of nodes (i.e. genes) and number of edges (i.e. gene interactions) in the network. A typical network size for most ChIP-Seq datasets is ~7400 nodes and ~7400 edges (note that most nodes have *degree* = 1), where each TF has several thousands of binding sites. A network of this size can be rendered in by VISIONET in less than one minute on our server.

A companion desktop version of VISIONET is available as a Microsoft Excel add-in. Since Excel is proprietary software, this desktop version is provided solely as an additional convenience to users, further to the web service.

The GraphML format enables users to work interchangeably between the web-based and desktop versions of VISIONET, and is convertible to the standard SBML format via the GraphMLReader plug-in for Cytoscape [24].

Results

Previously, VISIONET has been applied to the Gata4-Gata6 transcription factor network to discover *Hand2*, a developmental gene co-regulated by Gata4 and Gata6, being highly up-regulated in the adult cardiac fibroblasts [3]. Here, we applied VISIONET to construct cardiac fibroblast TF networks for Gata4 and Tbx20 (Figure 2A), two important cardiogenic TFs in heart development [25,26]. Not only have Gata4 and Tbx20 been shown to co-regulate important cardiac structure and functions during development [14,27] and in adult mice [28], we have made the recent surprising finding that both TFs are among the most highly up-regulated TFs in adult cardiac fibroblasts [13].

TFs have numerous gene targets, and frequently co-regulate gene expression. Identifying overlapping gene regulation, especially using visual approaches, is particularly interesting to biologists. In the case of cardiac function, the overlapping regions between the Gata4 and Tbx20 sub-networks are important for uncovering their largely unknown roles in the adult cardiac fibroblasts, because these two transcription factors are already known to co-regulate critical functions during heart development [14,15,27]. Existing platforms do not currently provide good solutions to this task. We illustrate this with the popular Cytoscape and CellDesigner platforms, which currently provide the most comprehensive libraries of layout methods. While VISIONET effectively visualises the overlapping target genes using its customised layout algorithm (Figure 2A), even the best empirical visual representations from Cytoscape (Figure 2B) and CellDesigner (Figure 2C) do not effectively display overlapping TF networks.

We used VISIONET to generate the overlapping TF networks of Tbx20 and Gata4, from the ChIP-Seq data (materials and methods described in Additional file 1: Text S1), and then overlaid our own microarray data of heart and tail fibroblasts [13] to highlight the expression levels; the resulting network can be seen in Figure 3A. To understand the heart-specific properties of cardiac fibroblasts, we must use fibroblasts from another organ as a reference. Together with cardiac fibroblasts, tail fibroblasts were previously reported to be reprogrammable into heart muscle cells [29]. This makes heart and tail fibroblasts important subjects for therapeutic applications in heart regeneration, and therefore highly interesting to compare.

A common feature of ChIP-Seq experiments is the thousands of ChIP-Seq peaks that are generated for each TF, leading to very large networks. The Gata4-Tbx20 co-regulation network contains 7434 nodes (Figure 3A). Without filtering, this network would be too dense and complex for human analysis (Figure 2A). We therefore used the VISIONET Log Fold Change (Log FC) filtering option to highlight genes that have at least 16-fold differences between heart and tail fibroblast expression levels. Genes that are up-regulated in the cardiac fibroblast relative to the tail fibroblast, i.e. Log FC > 4, were coloured solid red; genes that are relatively up-regulated in the tail fibroblast (Log FC < −4) were coloured solid blue; and all other genes are coloured grey and blurred out. This filtering and highlighting renders a human-readable graph, to which biologists can apply expert analysis (Figure 3A, solid nodes).

The filtered network revealed that out of the ~7400 genes in the entire network, only 13 genes (Additional file 1: Table S2) have 16-fold differences in expression between heart and tail fibroblasts, and are co-regulated by Tbx20 and Gata4. From these 13 genes, we then concentrated on the cardiogenic gene *Aldh1a2* (also known as *Raldh2*). The *Aldh1a2* gene stands out to cardiac experts because it uniquely displays three features: it is co-regulated by both Tbx20 and Gata4, it is more than 16-fold up-regulated in the cardiac fibroblasts compared to tail fibroblasts, and its mutation is known to be highly associated with diverse congenital heart disease phenotypes, including Tetralogy of

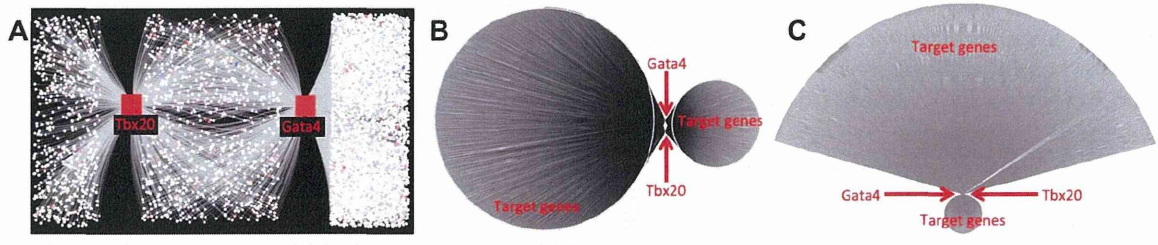

Figure 2 Comparison of VISIONET with the current state-of-art visualisation platforms, using the Gata4-Tbx20 case study. **(A)** Network using the customised VISIONET layout. **(B)** Network rending by Cytoscape using the "grouped by degree" layout (the most readable layout among other Cytoscape layouts in our empirical testing). **(C)** Network rending by CellDesigner using the "Circular" layout (the most readable layout among other CellDesigner layouts in our empirical testing).